



## Theoretical study of the stability of small triply charged carbon clusters $C_n^{3+}$ ( $n = 3-12$ )

G. Sánchez-Sanz<sup>a</sup>, S. Díaz-Tendero<sup>a,\*</sup>, F. Martín<sup>a,b</sup>, M. Alcamí<sup>a</sup>

<sup>a</sup> Departamento de Química, Módulo 13, Facultad de Ciencias, Universidad Autónoma de Madrid, 28049 Madrid, Spain

<sup>b</sup> Instituto Madrileño de Estudios Avanzados en Nanociencias (IMDEA-Nanociencia), Cantoblanco, 28049 Madrid, Spain

### ARTICLE INFO

#### Article history:

Received 10 June 2010

Received in revised form 3 September 2010

Accepted 3 September 2010

Available online 16 September 2010

#### Keywords:

Carbon cluster

Triply charged

Theoretical study

Dissociation energy

Ionization potential

### ABSTRACT

Using density functional theory, coupled cluster and multireference methods, dissociation energies and 3rd ionization potentials for, respectively, triply charged and neutral carbon clusters have been evaluated. The results show that the smaller  $C_n^{3+}$  clusters are metastable, i.e., they present a fragmentation channel with negative dissociation energy. The lowest dissociation channel always corresponds to evaporation of a singly charged carbon atom. Good agreement with available experimental data is found for most two-fragment channels. The third ionization potential of the corresponding neutral species decreases with cluster size.

© 2010 Elsevier B.V. All rights reserved.

### 1. Introduction

Small carbon clusters have been widely studied over the last two decades both theoretically and experimentally (see, e.g., the reviews [1–4]) due to their interest in astrophysical problems (see, e.g., [5–11]). Indeed, molecules exclusively formed by carbon atoms have been detected in the interstellar space and they have importance in the chemistry of carbon stars [12,13], comets [14], and interstellar molecular clouds [5,6,15–18]. Knowing the geometric, energetic and spectroscopic properties of these species is thus of great interest in order to interpret and analyze astrophysical data. In achieving this goal, theory has always played a fundamental role. Among the large number of theoretical studies devoted to neutral species, one must mention the work of Martin and coworkers [19–26]. Using high-level *ab initio* quantum chemistry methods, these authors have predicted structural, rotational, vibrational and electronic properties of neutral  $C_n$  clusters up to  $n = 18$ . Structural and spectroscopic properties of  $C_4$ ,  $C_5$  and  $C_6$  clusters have also been theoretically studied by Masso et al. [27–29]. Positively charged carbon clusters have been much less studied theoretically. Giufreda et al. [30] have used density functional theory (DFT) and coupled cluster (CC) methods to evaluate structural, rotational, vibrational, and electronic properties of linear and cyclic singly charged  $C_n^+$  clusters with  $n = 4-19$ . For small doubly charged carbon

clusters, multireference calculations were carried out by Hogreve, namely for  $C_2^{2+}$  [31],  $C_3^{2+}$  [32],  $C_4^{2+}$  [33] and  $C_5^{2+}$  [34]. In Ref. [35], this work was extended to larger  $C_n^{2+}$  clusters ( $n = 3-9$ ) by using DFT and CC methods. A semiempirical tight-binding model has also been employed for the study of neutral and (multi) charged clusters [36].

Fragmentation is the main deexcitation channel of highly excited carbon clusters [3,37,38]. Thus, to obtain information on the stability of these clusters, experimentalists have focused on the detection of the different fragments arising from neutral [39–41], singly negatively charged [42,43], singly positively charged [44–45], and multiply charged carbon clusters [41]. In the latter work, branching ratios for all the fragmentation channels resulting from the collision of swift  $C_n^+$  projectiles with noble gases were determined. As shown in Ref. [56], comparison of the measured fragmentation branching ratios with theoretical calculations allows one, in some cases, to extract the energy deposited in the collision. Very recently, the cluster internal energy resulting from the collision has been evaluated for carbon clusters  $C_n^{q+}$  with  $n = 5-10$  and  $q = 2-4$  [57].

Despite the experimental efforts to understand the stability of small highly charged carbon clusters, there is a lack of theoretical information for charges larger than +2. The aim of this paper is to provide energy data for small triply charged carbon clusters, such as dissociation energies, and the sequence of ionization potentials that lead to the triply charged species. The present data are thus of great importance to help in the interpretation of recent [58] and current experimental work on the fragmentation of  $C_n^{3+}$  clusters.

\* Corresponding author.

E-mail address: [sergio.diaztendero@uam.es](mailto:sergio.diaztendero@uam.es) (S. Díaz-Tendero).

These clusters are formed in collisions of singly charged  $C_n^+$  projectiles with noble gases, in which the former are doubly ionized and excited.

The paper is organized as follows. The theoretical methods used in our calculations are described in Section 2. Results and discussion are presented in Section 3. Comparison between our results and recent experimental data is also included. We end with some conclusions in Section 4.

## 2. Computational details

In the present work we have used different methodologies for the description of triply charged small carbon clusters: DFT, CC method, Complete Active Space Self Consistent Field (CASSCF) and Complete Active Space Self Consistent Field including second-order perturbation theory (CASPT2).

For the DFT calculations, we have chosen the B3LYP functional which combines the Becke's three parameter nonlocal hybrid exchange potential [59] with the nonlocal correlation functional of Lee et al. [60].  $C_n^{3+}$  clusters are open-shell systems, i.e., they have unpaired electrons and the unrestricted density functional theory (UDFT) has been used. In a previous work [35], we selected this functional for the description of doubly charged small carbon clusters showing that the results obtained are in good agreement with CC results. In addition, this functional has been previously used with success in the description of dissociation energies and fission barriers of (highly) charged fullerenes [61–65]. We thus consider that B3LYP is a reasonable choice; we have used it in combination with the 6-311+G(3df) basis set, which is a triple split valence basis, supplemented with a diffuse function (+), and three d-type and one f-type polarization functions. B3LYP/6-311+G(3df) has been used in the geometry optimization of all the species considered in this work.

Coupled cluster calculations, including single and double excitations, and triple excitations in a perturbative way, CCSD(T), have been carried out over the DFT optimized geometries (obtained at the B3LYP/6-311+G(3df) level) to obtain more accurate values of the energy.

DFT and CC methods are based on a single-reference wave function. To complement the theoretical description and to better understand the results obtained, we have also performed calculations for the smaller clusters using a multireference based approach. In particular, we have carried out calculations using the CASSCF method, which includes non dynamical correlation. In a second step, we have included the electronic dynamic correlation in the CASSCF wave function within the second-order perturbation theory (CASPT2). CASSCF calculations in combination with the same 6-311+G(3df) basis set have also been used to optimize the geometry of the smaller clusters. Single point CASPT2/6-311+G(3df) calculations were carried out to obtain a more accurate value of the energies. In these multireference methodologies, the choice of the active space is crucial. We have used the following selected active spaces (number of electrons, number of orbitals): (5,6) and (7,9) for  $C_3^{3+}$  and  $C_4^{3+}$ , respectively. Thus in CASSCF and CASPT2 calculations all valence electrons were correlated.

DFT and CCSD(T) calculations were performed with the Gaussian03 package [66] and the CASSCF and CASPT2 ones with the MOLPRO program [67].

## 3. Results and discussion

Theoretical results for carbon clusters may present serious deficiencies when single-reference methods are used. It has been shown that static correlation may be important in these systems and DFT methods often yield to instabilities in the wavefunction

(symmetry breaking, internal instabilities or RHF  $\rightarrow$  UHF instabilities) or very large spin contaminations [35]. CCSD(T) also presents serious deficiencies in some particular cases, reflected in very large values of the T1 diagnostic [35]. The multireference calculations have allowed us to: (i) analyze the instabilities and spin contamination problems that may appear in DFT calculations, (ii) obtain a deeper understanding on the wave function properties, and (iii) investigate the multiconfigurational nature of  $C_n^{3+}$  clusters. In addition, a systematic study of the stability of different isomers, their geometry, and vibrational frequencies was carried out. A detailed analysis of these technical aspects are beyond the scope of the present work and will be published elsewhere [68]. In this article, we will focus on the results of experimental interest and, from the comparison between the different theoretical methods, we will be able to show the accuracy that can be expected from our calculated data.

### 3.1. Ionization potentials

Third ionization potentials have been evaluated at the B3LYP/6-311+G(3df) and CCSD(T)/6-311+G(3df)//B3LYP/6-311+G(3df) levels for cluster size up to  $n=12$ . The results are presented in Fig. 1 together with the first and second ionization potentials taken from previous work [35]. Since, in the latter work, results were only reported for  $C_n$  clusters with sizes up to  $n=9$ , for completeness, in the present work, we have extended the calculations of first and second ionization potentials up to  $n=12$  (see Fig. 1). CASSCF and CASPT2 calculations have been restricted to clusters with four or less atoms. It can be seen that DFT leads to first and second IPs that are  $\sim 0.4$  and  $\sim 0.8$  eV, respectively, above the CCSD(T) results. In contrast, it leads to third IPs  $\sim 0.7$  eV below the CCSD(T) results. The ionization potentials resulting from the CASSCF and CASPT2 calculations differ by less than 1 eV in most cases.

As already discussed in [35], the first IP decreases very slowly with cluster size. In contrast, the second ionization potential decreases rapidly with the number of atoms. Our calculations show that this is also the case for the third IP, since the larger the cluster the easier the charge is accommodated.

### 3.2. Dissociation energies

In this case CASSCF and CASPT2 calculations have been restricted to clusters with four or less atoms and to fragmentation channels corresponding to evaporation of a neutral or a charged monomer. Fig. 1 shows the corresponding dissociation energies obtained with the different methods.<sup>1</sup> In general, a reasonable agreement between multireference methods and DFT is obtained. As a general rule, multireference methods lead to slightly lower dissociation energies than single-reference methods (DFT and CCSD(T)). However, the observed general trends are basically the same for all dissociation channels investigated here. The differences between DFT and CCSD(T) results are of the order of 1 eV and, in most cases, the former are slightly above the latter.

Being confident that the DFT-B3LYP approach leads to reasonable results, we have extended the above calculations to all the possible two-fragment dissociation channels:  $C_n^{3+} \rightarrow C_{n-x}^{(3-q)+} + C_x^{q+}$ . The results are shown in Fig. 2 as function of the size of the original cluster,  $n$ . As a general trend, the dissociation energy for the ejection of a neutral fragment [ $C_n^{3+} \rightarrow C_{n-x}^{3+} + C_x$ ] decreases with cluster size, while for the other channels [ $C_n^{3+} \rightarrow C_{n-x}^{(3-q)+} + C_x^{q+}$ ,  $q > 0$ ] it increases rather monotonically. This can be explained in terms of

<sup>1</sup>  $C_2^{3+}$  is unstable in its ground state: it dissociates without barrier in  $C_2^+ + C^+$  due to Coulomb explosion and, therefore, it cannot be detected experimentally. Thus, the dissociation energy of the channels involving  $C_2^{3+}$  is not given.

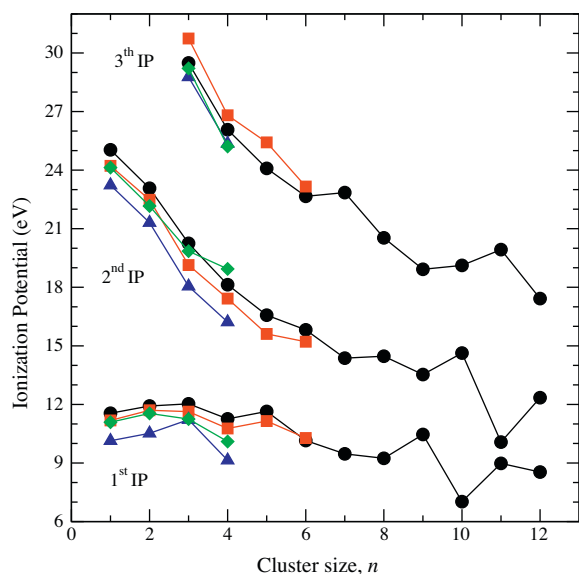


**Fig. 1.** Ionization potentials (IPs) for  $C_n$  clusters evaluated at different levels of theory: B3LYP/6-311+G(3df)—black circles, CCSD(T)/6-311+G(3df)//B3LYP/6-311+G(3df)—red squares, CASSCF/6-311+G(3df)—blue triangles and CASPT2/6-311+G(3df)//CASSCF/6-311+G(3df)—green diamonds. 1st, 2nd IP and, 3rd IP are indicated in the figure. (For interpretation of the references to colour in this figure legend, the reader is referred to the web version of the article.)

charge sharing and taking into account that the stability of the final fragments decreases when the charge is located in the smaller fragment. Thus, in the case of ejection of a neutral fragment (Fig. 3a), all the curves decrease irrespective of the value of  $x$  because the whole charge ( $q = 3$ ) is located in the larger fragment and this becomes progressively more stable as  $n$  increases. Comparing the dissociation energies for a particular value of  $n$ , we observe that they increase as

$x$  increases, since now the charge is located in progressively smaller fragments (thus, less stable products). When the charge is shared between both fragments (Fig. 3b and c), the most stable products are, therefore, the lower dissociation energies correspond to those cases in which the double charge is located in the larger fragment. This explains why in Fig. 3b the general trend is an increase of the dissociation energy with  $n$  and with  $x$ , while in Fig. 3c the dissociation energy increases with  $n$  but decreases with  $x$ . Finally, Fig. 3d considers the case in which the charge is located in the smaller fragment. As expected the dissociation energies increase with  $n$  and decrease with  $x$ .

The global picture that can be obtained from all the results shown in Fig. 3 is that fission channels, in which the charge is shared by the two fragments, are the most favorable fragmentation channels. Indeed, the lowest dissociation energies are obtained in panel b, i.e., when the smaller fragment holds a charge of +1 and the larger one a charge of +2. In particular, ejection of  $C^+$  is the most favorable process. This is at variance with the results reported for singly- [69] and doubly-charged [35] small carbon clusters, for which evaporation of a neutral trimer has the lowest dissociation energy. This is because  $C_3$  has an unusually high stability [70]. However this is not enough to compensate the strong Coulomb repulsion that would exist in the remaining triply charged cluster.

Our theoretical predictions also show that all the  $C_n^{3+}$  clusters studied in this work, except for  $C_{10}^{3+}$  and  $C_{11}^{3+}$ , present a fragmentation channel with a dissociation energy lower than zero. This implies that triply charged carbon clusters are thermodynamically unstable. However, the channels for which dissociation energies are negative are precisely those associated with asymmetric fission. As is well known, fission channels are always associated with barriers in the potential energy surface, which prevent the system from spontaneously dissociating. Hence, triply charged carbon clusters are in fact metastable species. Fission barriers have also been observed in small doubly charged carbon clusters [31–34] and highly charged fullerenes [61,62].

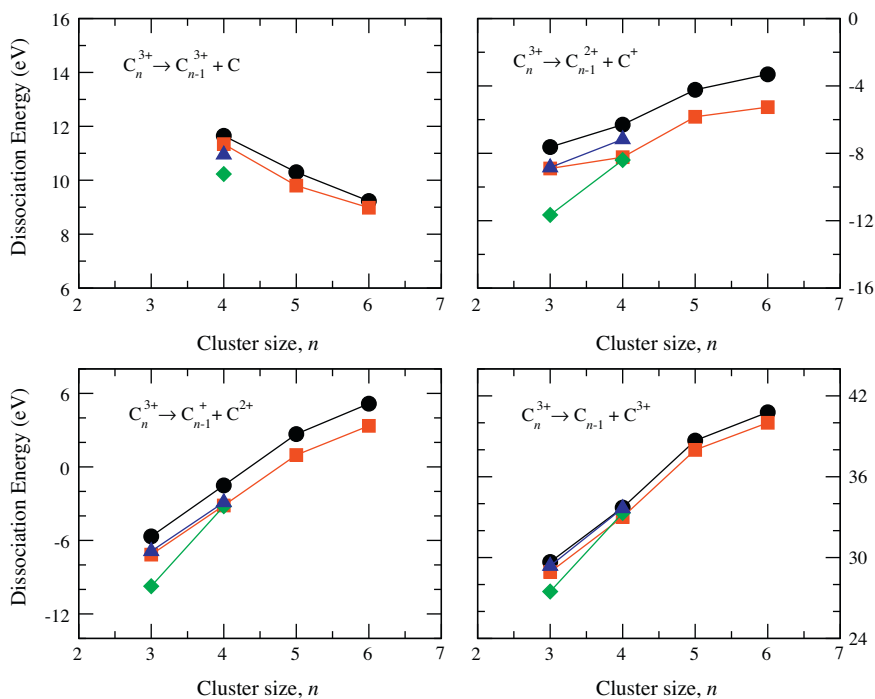


**Fig. 2.** Dissociation energies for  $C_n^{3+}$  clusters evaluated at the different levels of theory: B3LYP/6-311+G(3df)—black circles, CCSD(T)/6-311+G(3df)//B3LYP/6-311+G(3df)—red squares, CASSCF/6-311+G(3df)—blue triangles and CASPT2/6-311+G(3df)//CASSCF/6-311+G(3df)—green diamonds. Upper-left panel:  $C_n^{3+} \rightarrow C_{n-1}^{3+} + C$ ; upper-right panel:  $C_n^{3+} \rightarrow C_{n-1}^{2+} + C^+$ ; bottom-left panel:  $C_n^{3+} \rightarrow C_{n-1}^+ + C^{2+}$ ; bottom-right panel:  $C_n^{3+} \rightarrow C_{n-1} + C^{3+}$ . (For interpretation of the references to colour in this figure legend, the reader is referred to the web version of the article.)

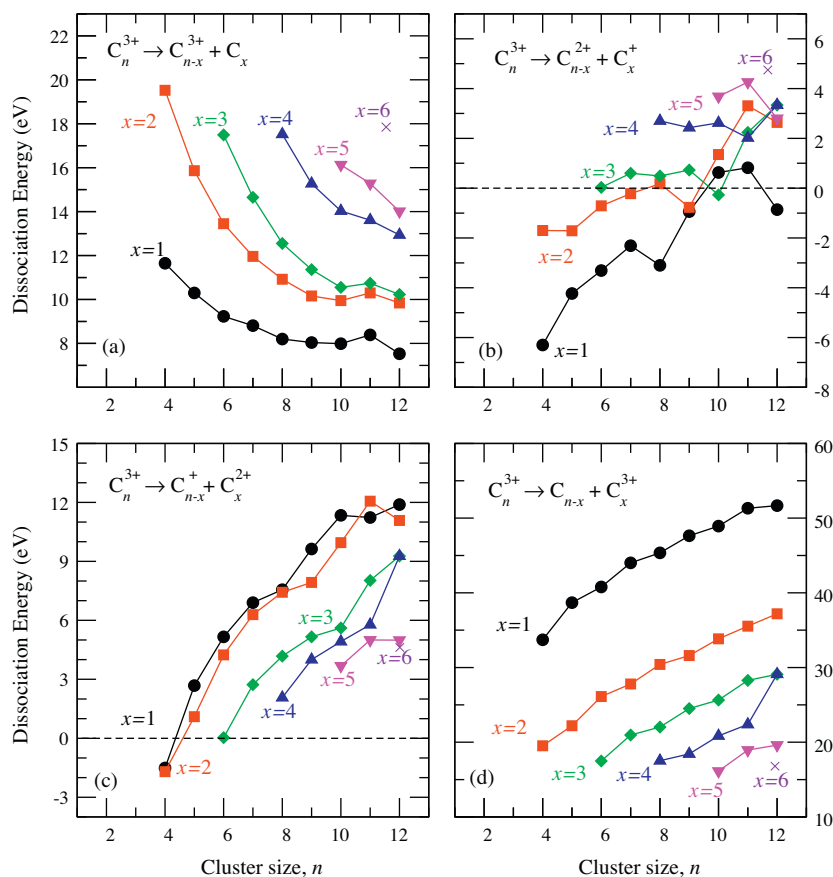


**Fig. 3.** Dissociation energies of  $C_n^{3+}$  clusters calculated at the B3LYP/6-311+G(3df) level of theory. Top-left panel: evaporation of  $C_x$ ; top-right panel: evaporation of  $C_x^+$ ; bottom-left panel: evaporation of  $C_x^{2+}$  and bottom-right panel: evaporation of  $C_x^{3+}$ .  $x=1$ , black circles;  $x=2$ , red squares;  $x=3$ , green diamonds;  $x=4$ , blue triangles up;  $x=5$ , magenta triangles down;  $x=6$  violet cross. (For interpretation of the references to colour in this figure legend, the reader is referred to the web version of the article.)

The fact that the most favorable channel (i.e., the one with the lowest dissociation energy) corresponds to  $C_n^{3+} \rightarrow C_{n-1}^{2+} + C^+$  suggests that this should be the dominant fragmentation channel, in agreement with the existing experiments [58]. As an illustration, we compare in Table 1 the experimental branching ratios [58] with the calculated dissociation energies for the most relevant fragmentation channels in  $C_5^{3+}$ . As the energy deposited in the experiment is of the order of 10 eV [41,56,57], fragmentation leading to more than two fragments is possible. For these multifragmentation channels, we also report the corresponding dissociation energies in Table 1. In the case of two fragments, the lowest dissociation energy corresponds to  $C_5^{3+} \rightarrow C_4^{3+} + C^+$ , followed by  $C_5^{3+} \rightarrow C_3^{2+} + C_2^+$  and then by  $C_5^{3+} \rightarrow C_4^+ + C_2^+$ . As can be seen in Table 1, the experimental branching ratios decrease accordingly. For the case of  $C_6^{3+}$  (results not shown in the table), the calculated dissociation energies predict the following order of decreasing branching ratios:  $C_6^{3+} \rightarrow C_5^{2+} + C^+$  followed by  $C_6^{3+} \rightarrow C_4^{2+} + C_2^+$  and then by  $C_6^{3+} \rightarrow C_3^{2+} + C_3^+$ . The experimental values are [58]  $4.4 \pm 0.4\%$ ,  $0.2 \pm 0.1\%$  and  $0.5 \pm 0.04\%$ , respectively. Therefore, theory correctly predicts that the most favorable process is ejection of a singly charged monomer. With very few exceptions, a similar correlation between measured branching ratios and calculated dissociation energies is obtained for three, four and five fragment ejection. However, the correlation does not hold so well when one compares branching ratios corresponding to channels with a different number of fragments.

Fig. 4 shows the experimental branching ratios as functions of dissociation energies for the two-fragment channels  $C_n^{3+} \rightarrow C_{n-x}^{(3-q)+} + C_x^{q+}$  ( $n=5-10$ ). The calculated data can be found in Table 1 of the Appendix. As can be seen, the largest branching

ratios correspond to the smallest dissociation energies. There is however a significant dispersion of the points with respect to an exponential fit. This dispersion indicates that other effects, apart from the dissociation energy, are important in the fragmentation

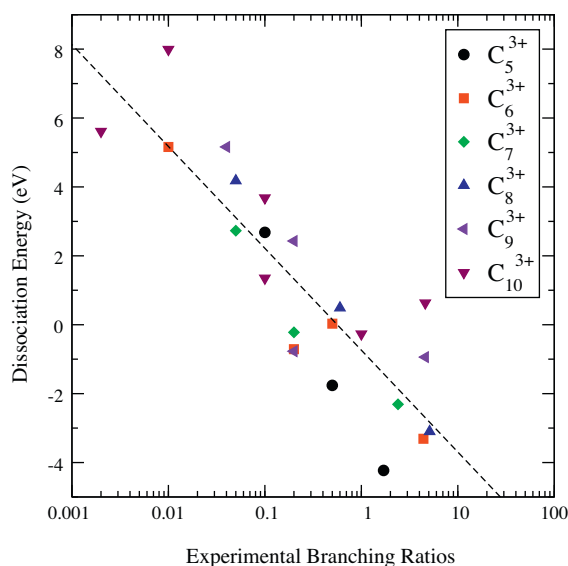


**Fig. 4.** Dissociation energies as functions of experimental branching ratios for the two-fragment channels  $C_n^{3+} \rightarrow C_{n-x}^{(3-q)+} + C_x^{q+}$ ;  $n=5$ , circles;  $n=6$ , squares;  $n=7$ , diamonds;  $n=8$ , triangles up;  $n=9$ , triangles left;  $n=10$ , triangles down. Dashed line: exponential fit  $BR_i = \exp[-(DE_i (\text{eV}) + 0.7387/1.2841)]$ , where  $DE_i$  is the dissociation energy associated with the fragmentation channel  $i$ ;  $\chi^2 = 0.746$ .

**Table 1**  
Experimental branching ratios from Ref. [58] compared to dissociation energies calculated at the B3LYP and CCSD(T) levels for  $C_5^{3+}$ .

Number of fragments	Fragmentation channel	Experimental branching ratio (error)	Dissociation energy (eV)	
			B3LYP(eV)	CCSD(T)
2	$C_4^{2+}/C$	1.70 ( $\pm 0.2$ )	-4.23	-5.83
	$C_3^{2+}/C_2^+$	0.50 ( $\pm 0.06$ )	-1.71	-3.89
	$C_4^+/C_2^{2+}$	0.10 ( $\pm 0.02$ )	2.68	0.97
3	$C_3^+/C^+/C^+$	16.70 ( $\pm 1$ )	-4.71	-6.39
	$C_2^+/C_2^+/C^+$	7.10 ( $\pm 1$ )	-2.93	-4.53
	$C_3^{2+}/C^+/C$	0.30 ( $\pm 0.05$ )	4.00	2.67
4	$C_2^+/C^+/C^+/C$	23.90 ( $\pm 2$ )	2.79	0.84
	$C_2/C^+/C^+/C^+$	7.90 ( $\pm 0.6$ )	2.41	0.30
	$C_2^+/C_2^{2+}/C/C$	0.20 ( $\pm 0.03$ )	16.28	13.88
5	$C^+/C^+/C^+/C/C$	40.10 ( $\pm 2$ )	8.50	6.40
	$C^{2+}/C^+/C/C/C$	0.90 ( $\pm 0.1$ )	21.99	19.44

**Table A.1**  
Dissociation energies (in eV) for all possible two-fragment channels  $C_n^{3+} \rightarrow C_{n-x}^{(3-q)+} + C_x^{q+}$  evaluated at the B3LYP/6-311+G(3df) level. Results in brackets correspond to the CCSD(T)/6-311+G(3df)//B3LYP/6-311+G(3df) level of theory.

$n-1$								
$n$	$C_n^{3+} \rightarrow C_{n-1}^{3+} + C$		$C_n^{3+} \rightarrow C_{n-1}^{2+} + C^+$		$C_n^{3+} \rightarrow C_{n-1}^+ + C_2^{2+}$		$C_n^{3+} \rightarrow C_{n-1} + C_3^{3+}$	
3			-7.63	(-8.90)	-5.67	(-7.16)	29.67	(28.93)
4	11.65	(11.34)	-6.30	(-8.23)	-1.51	(-3.15)	33.71	(33.01)
5	10.30	(9.80)	-4.23	(-5.83)	2.68	(0.97)	38.68	(37.99)
6	9.23	(8.93)	-3.31	(-5.26)	5.16	(3.35)	40.78	(40.00)
7	8.81	(8.33)	-2.31	(-3.65)	6.90	(5.36)	44.01	(42.87)
8	8.20	(8.17)	-3.10	(-4.31)	7.56	(9.84)	45.35	(44.71)
9	8.04	(7.35)	-0.94		9.63	(10.63)	47.64	(46.61)
10	7.99		0.63		11.34		48.93	
11	8.39		0.82		11.23		51.32	
12	7.53		-0.86		11.89		51.67	
$n-2$								
$n$	$C_n^{3+} \rightarrow C_{n-2}^{3+} + C_2$		$C_n^{3+} \rightarrow C_{n-2}^+ + C_2^+$		$C_n^{3+} \rightarrow C_{n-2} + C_2^{3+}$			
4			-1.70	(-3.03)	-1.70		(-3.03)	
5	15.86	(15.15)	-1.71	(-3.89)	1.10		(-0.55)	
6	13.45	(12.80)	-0.71	(-2.31)	4.24		(2.74)	
7	11.96	(11.32)	-0.22	(-2.39)	6.29		(4.48)	
8	10.92	(10.51)	0.18	(-0.94)	7.43		(6.32)	
9	10.16	(9.54)	-0.77	(-2.42)	7.93		(10.00)	
10	9.95		1.35		9.95			
11	10.30		3.31		12.06			
12	9.84		2.64		11.08			
$n-2$								
$n$	$C_n^{3+} \rightarrow C_{n-3}^{3+} + C_3$		$C_n^{3+} \rightarrow C_{n-3}^{2+} + C_3^+$		$C_n^{3+} \rightarrow C_{n-3}^+ + C_3^{2+}$		$C_n^{3+} \rightarrow C_{n-3} + C_3^{3+}$	
6	17.49	(16.87)	0.03	(-2.23)	0.03	(-2.23)	17.49	(16.87)
7	14.65	(13.87)	0.60	(-1.31)	2.73	(0.41)	20.97	(20.38)
8	12.55	(12.24)	0.49	(-1.55)	4.18	(1.99)	22.03	(21.58)
9	11.36	(10.61)	0.73	(-0.91)	5.16	(3.02)	24.50	(23.48)
10	10.55		-0.27		5.61		25.64	
11	10.74		2.24		8.03		28.28	
12	10.23		3.34		9.27		29.10	
$n-4$								
$n$	$C_n^{3+} \rightarrow C_{n-4}^{3+} + C_4$		$C_n^{3+} \rightarrow C_{n-4}^{2+} + C_4^+$		$C_n^{3+} \rightarrow C_{n-4}^+ + C_4^{2+}$		$C_n^{3+} \rightarrow C_{n-4} + C_4^{3+}$	
8	17.52	(17.22)	2.70	(1.18)	2.70	(1.18)	17.52	(17.22)
9	15.27	(14.77)	2.43	(0.12)	4.00	(1.94)	18.43	(17.60)
10	14.03		2.62		4.92		20.85	
11	13.61		2.02		5.78		22.38	
12	12.94		3.34		9.27		29.10	
$n-5$								
$n$	$C_n^{3+} \rightarrow C_{n-5}^{3+} + C_5$		$C_n^{3+} \rightarrow C_{n-5}^{2+} + C_5^+$		$C_n^{3+} \rightarrow C_{n-5}^+ + C_5^{2+}$		$C_n^{3+} \rightarrow C_{n-5} + C_5^{3+}$	
10		16.13		3.68		3.68		16.13
11		15.28		4.26		5.00		18.95
12		14.01		2.80		4.99		19.61
$n-6$								
$n$	$C_n^{3+} \rightarrow C_{n-6}^{3+} + C_6$		$C_n^{3+} \rightarrow C_{n-6}^{2+} + C_6^+$		$C_n^{3+} \rightarrow C_{n-6} + C_6^{2+}$		$C_n^{3+} \rightarrow C_{n-6} + C_6^{3+}$	
12		17.24		4.72		4.72		17.24

process, e.g., entropy or fission barriers. Inclusion of the latter in the few cases where this was possible leads, in general, to more realistic predictions [70,71].

#### 4. Conclusions

In this work we have presented a theoretical study of third ionization potentials and dissociation energies of, respectively, neutral  $C_n$  and triply charged  $C_n^{3+}$  clusters with sizes  $n = 3–12$  using methods based on single-reference (DFT and CCSD(T)) and multireference (CASSCF and CASPT2) wave functions. We have shown that the third ionization potential decreases with cluster size, following a behavior similar to that of the second ionization potential. Dissociation energies for all the possible fragmentation channels have been evaluated. The results show that the channel with the lowest dissociation energy corresponds to evaporation of a singly charged carbon atom:  $C_n^{3+} \rightarrow C_{n-1}^{2+} + C^+$ . They also show that triply charged carbon clusters are metastable, i.e., they correspond to local (not global) minima in the potential energy surface which are separated from the dissociation products by Coulomb barriers. The conclusions are the same for the four methods used in this work. In particular, the reasonable agreement between DFT and CASSCF results for both ionization potentials and dissociation energies suggests that DFT is a reasonable choice to the study larger carbon clusters (including highly charged fullerenes) for which a multireference treatment becomes prohibitively expensive.

#### Acknowledgements

S.D.-T. gratefully acknowledges the Juan de la Cierva program of the Spanish Ministerio de Educación y Ciencia. We acknowledge a generous allocation of computer time at the Centro de Computación Científica at the Universidad Autónoma de Madrid (CCC-UAM). This work was supported by the DGI Projects FIS2007-60064 and CSD 2007-00010, and the CAM project S2009/MAT1726.

#### Appendix A. Dissociation energies

Table A.1 shows the dissociation energies for all possible two-fragment channels  $C_n^{3+} \rightarrow C_{n-x}^{(3-q)+} + C_x^{q+}$  evaluated at the B3LYP/6-311+G(3df) and CCSD(T)/6-311+G(3df)//B3LYP/6-311+G(3df) levels of theory.

#### References

- [1] W. Weltner, R.J.V. Z33, *Chem. Rev.* 89 (1989) 1713.
- [2] A.V. Orden, R.J. Saykally, *Chem. Rev.* 98 (1998) 2313.
- [3] C. Lifshitz, *Int. J. Mass Spectrom.* 200 (2000) 423.
- [4] M. Bianchetti, P. Buonsante, F. Ginelli, H. Roman, R. Broglia, F. Alasia, *Phys. Rep.* 357 (2002) 459.
- [5] R.P.A. Bettens, E. Herbst, *Astrophys. J.* 468 (1996) 686.
- [6] R.P.A. Bettens, E. Herbst, *Astrophys. J.* 478 (1997) 585.
- [7] S.S. Seahra, W.W. Duley, *Astrophys. J.* 520 (1999) 719.
- [8] J. Cernicharo, J.R. Goicoechea, Y. Benilan, *Astrophys. J.* 580 (2002) L157.
- [9] J.R. Goicoechea, J. Cernicharo, H. Masso, M.L. Senent, *Astrophys. J.* 609 (2004) 225.
- [10] J. Pety, D. Teyssier, D. Fossé, M. Gerin, E. Roueff, A. Abergel, E. Habart, J. Cernicharo, *Astron. Astrophys.* 435 (2005) 885–899.
- [11] J. Cernicharo, M. Guélin, M. Agúndez, K. Kawaguchi, M. McCarthy, P. Thaddeus, *Astron. Astrophys.* 467 (2007) L37–L40.
- [12] K.W. Hinkle, J.J. Keady, P.F. Bernath, *Science* 241 (1988) 1319.
- [13] P.F. Bernath, K.H. Hinkle, J.J. Keady, *Science* 244 (1989) 562.
- [14] A.E. Douglas, *Astrophys. J.* 114 (1951) 466.
- [15] A.V. Orden, J.D. Cruzan, R.A. Provencal, T.F. Giesen, R.J. Saykally, R.T. Boreiko, A.L. Betz, *Proceedings of the Airborne Astronomy Symposium on the Galactic Ecosystem*, vol. 73, APS Conference Series, The Astronomical Society of the Pacific, San Francisco, 1995.
- [16] L.M. Haffner, D.M. Meyer, *Astrophys. J.* 453 (1995) 450.
- [17] D.E. Woon, E. Herbst, *Astrophys. J.* 465 (1996) 795–799.
- [18] D.P. Ruffle, R.P.A. Bettens, R. Terzieva, E. Herbst, *Astrophys. J.* 523 (1999) 678.
- [19] J.M.L. Martin, J.P. François, R. Gijbels, *J. Chem. Phys.* 93 (1990) 8850.

- [20] J.M.L. Martin, J.P. François, R. Gijbels, *J. Chem. Phys.* 94 (1991) 3753.
- [21] J.M.L. Martin, P.R.J. Taylor, *J. Chem. Phys.* 102 (1995) 8270.
- [22] J.M.L. Martin, J. El-Yazal, J.P. François, *Chem. Phys. Lett.* 242 (1995) 570.
- [23] J.M.L. Martin, P.R. Taylor, *Chem. Phys. Lett.* 240 (1995) 521.
- [24] J.M.L. Martin, P.R.J. Taylor, *J. Phys. Chem.* 100 (1996) 6047.
- [25] J.M.L. Martin, J. El-Yazal, J.P. François, *Chem. Phys. Lett.* 252 (1996 a) 9.
- [26] J.M.L. Martin, D.W. Schwenke, T.J. Lee, P.R. Taylor, *J. Chem. Phys.* 104 (1996 b) 4657.
- [27] H. Masso, M. Senent, P. Rosmus, M. Hochlaf, *J. Chem. Phys.* 124 (2006) 234304.
- [28] H. Masso, V. Vervazov, P. Malmqvist, B. Roos, M. Senent, *J. Chem. Phys.* 127 (2007) 154318.
- [29] H. Masso, M. Senent, *J. Phys. Chem. A* 113 (2009) 12404.
- [30] M.G. Giuffreda, M.S. Deleuze, J.P. François, *J. Phys. Chem. A* 103 (1999) 5137.
- [31] H. Hogreve, *Chem. Phys.* 202 (1996) 63.
- [32] H. Hogreve, *J. Chem. Phys.* 102 (1995) 3281.
- [33] H. Hogreve, *J. Mol. Struct. (Theochem.)* 532 (2000) 81.
- [34] H. Hogreve, A.F. Jalbout, *J. Chem. Phys.* 119 (2003) 8849.
- [35] S. Díaz-Tendero, F. Martín, M. Alcamí, *J. Phys. Chem. A* 106 (2002) 10782.
- [36] L. Montagnon, F. Spiegelman, *J. Chem. Phys.* 127 (2007) 084111.
- [37] E.E.B. Campbell, F. Rohmund, *Rep. Prog. Phys.* 63 (2000) 1061.
- [38] E.E. Campbell, *Fullerene Collision Reactions*, 1st ed., Kluwer Academic Publishers, Dordrecht, 2003.
- [39] H. Choi, R.T. Bise, A.A. Hoops, D.H. Mordant, D.M. Neumark, *J. Phys. Chem.* 104 (2000) 2025.
- [40] M. Chabot, S.D. Negra, L. Lavergne, G. Martinet, K. Wohrer, R. Sellem, R. Daniel, J.L. Bris, G. Lahu, D. Gardés, J.A. Scarpati, P. Désesquelles, V. Lima, *Nucl. Instrum. Meth. B* 197 (2002) 155.
- [41] K. Beroff, M. Chabot, F. Mezdari, G. Martinet, T. Tuna, P. Desesquelles, A. LePardellec, M. Barat, *Nucl. Inst. Meth. Phys. Res. Sec. B: Beam Interact. Mater. At.* 267 (2009) 866.
- [42] S.W. McElvany, *Int. J. Mass Spectrom. Ion Proc.* 102 (1990) 81.
- [43] Y. Tai, J. Murakami, Y. Maruyama, W. Yamaguchi, T. Mizota, K. Igarashi, S. Tanemura, *J. Phys. Chem. B* 103 (1999) 5500.
- [44] P.P. Radi, T.L. Bunn, P. Kemper, M.E. Molchan, M.T. Bowers, *J. Chem. Phys.* 88 (1988) 2809.
- [45] P.P. Radi, M.E. Rincon, M.T. Hsu, J. Brodbelt-Lustig, P. Kemper, M.T. Bowers, *J. Chem. Phys.* 93 (1989) 6187.
- [46] P.P. Radi, M.E. Rincon, M.T. Hsu, J. Brodbelt-Lustig, P.R. Kemper, M.T. Bowers, *J. Chem. Phys.* 92 (1990) 4817.
- [47] P.P. Radi, G.V. Helden, M.T. Hsu, P.R. Kemper, M.T. Bowers, *Int. J. Mass Spectrom. Ion Proc.* 109 (1991) 49.
- [48] M.E. Geusic, T.J. McIlrath, M.F. Jarrold, L.A. Bloomfield, R.R. Freeman, W.L. Brown, *J. Chem. Phys.* 84 (1986) 2421.
- [49] M.E. Geusic, T.J. McIlrath, M.F. Jarrold, L.A. Bloomfield, R.R. Freeman, W.L. Brown, *Z. Phys. D* 3 (1986) 309.
- [50] M.E. Geusic, M.F. Jarrold, T.J. McIlrath, R.R. Freeman, W.L. Brown, *J. Chem. Phys.* 86 (1987) 3862.
- [51] R. Bouyer, F.R. Monchicourt, M. Perdix, P. Pradel, *J. Chem. Phys.* 100 (1994) 8912.
- [52] K.B. Shelimov, J.M. Hunter, M.F. Jarrold, *Int. J. Mass Spectrom. Ion Proc.* 138 (1994) 17.
- [53] M.B. Sowa, P.A. Hinz, S.L. Anderson, *J. Chem. Phys.* 95 (1991) 4719.
- [54] C. Lifshitz, T. Peres, I. Agranat, *Int. J. Mass Spectrom. Ion Proc.* 93 (1989) 149.
- [55] C. Lifshitz, H.F.G.P. Sandler, J. Sun, T. Weiske, H. Schwart, *J. Phys. Chem.* 97 (1993) 6592.
- [56] G. Martinet, S. Díaz-Tendero, M. Chabot, K. Wohrer, S.D. Negra, F. Mezdari, H. Hamrita, P. Désesquelles, A.L. Padellec, D. Gardés, L. Lavergne, G. Lahu, X. Grave, J.F. Clavelin, P.A. Hervieux, M. Alcamí, F. Martín, *Phys. Rev. Lett.* 93 (2004) 063401.
- [57] M. Chabot, F. Mezdari, K. Béroff, G. Martinet, P.-A. Hervieux, *Phys. Rev. Lett.* 104 (2010) 043401.
- [58] F. Mezdari, *Fragmentation d'agrégats de carbone (multi) chargés formés par ionisation et excitation en collision de haute vitesse*, Ph.D. Thesis, Université Paris-Sud, Orsay, 2005.
- [59] A.D. Becke, *J. Chem. Phys.* 98 (1993) 5648.
- [60] C. Lee, W. Yang, R.G. Parr, *Phys. Rev. B* 37 (1988) 785.
- [61] S. Díaz-Tendero, M. Alcamí, F. Martín, *Phys. Rev. Lett.* 95 (2005) 013401.
- [62] S. Díaz-Tendero, M. Alcamí, F. Martín, *J. Chem. Phys.* 123 (2005) 184306.
- [63] G. Sánchez, S. Díaz-Tendero, F. Martín, M. Alcamí, *Chem. Phys. Lett.* 416 (2005) 14.
- [64] S. Díaz-Tendero, G. Sánchez, M. Alcamí, F. Martín, *Int. J. Mass Spectrom.* 252 (2006) 133–141.
- [65] H. Zettergren, G. Sánchez, S. Díaz-Tendero, M. Alcamí, F. Martín, *J. Chem. Phys.* 127 (2007) 2007.
- [66] M.J. Frisch, G.W. Trucks, H.B. Schlegel, G.E. Scuseria, M.A. Robb, J.R. Cheeseman, J.A. Montgomery, Jr., T. Vreven, K.N. Kudin, J.C. Burant, J.M. Millam, S.S. Iyengar, J. Tomasi, V. Barone, B. Mennucci, M. Cossi, G. Scalmani, N. Rega, G.A. Petersson, H. Nakatsuji, M. Hada, M. Ehara, K. Toyota, R. Fukuda, J. Hasegawa, M. Ishida, T. Nakajima, Y. Honda, O. Kitao, H. Nakai, M. Klene, X. Li, J.E. Knox, H.P. Hratchian, J.B. Cross, V. Bakken, C. Adamo, J. Jaramillo, R. Gomperts, R.E. Stratmann, O. Yazyev, A.J. Austin, R. Cammi, C. Pomelli, J.W. Ochterski, P.Y. Ayala, K. Morokuma, G.A. Voth, P. Salvador, J.J. Dannenberg, V.G. Zakrzewski, S. Dapprich, A.D. Daniels, M.C. Strain, O. Farkas, D.K. Malick, A.D. Rabuck, K. Raghavachari, J.B. Foresman, J.V. Ortiz, Q. Cui, A.G. Baboul, S. Clifford, J. Cioslowski, B.B. Stefanov, G. Liu, A. Liashenko, P. Piskorz, I. Komaromi, R.L. Martin, D.J. Fox, T. Keith, M.A. Al-Laham, C.Y. Peng, A. Nanayakkara, M. Challacombe, P.M.W. Gill, B. John-

- son, W. Chen, M. W. Wong, C. Gonzalez, J.A. Pople, Gaussian03, Revision E.01, Gaussian, Inc., Wallingford, CT, 2004.
- [67] H.-J. Werner, P.J. Knowles, R. Lindh, M. Schütz, P. Celani, T. Korona, F.R. Manby, G. Rauhut, R.D. Amos, A. Bernhardsson, A. Berning, D.L. Cooper, M.J.O. Deegan, A.J. Dobbyn, F. Eckert, C. Hampel, G. Hetzer, A.W. Lloyd, S.J. McNicholas, W. Meyer, M.E. Mura, A. Nicklass, P. Palmieri, R. Pitzer, U. Schumann, H. Stoll, A.J. Stone, R. Tarroni, T. Thorsteinsson, Molpro, Version 2002.6, A Package of ab initio Programs, 2003, <http://www.molpro.net>.
- [68] G. Sánchez-Sanz, S. Díaz-Tendero, F. Martín, M. Alcamí, to be submitted.
- [69] S. Díaz-Tendero, G. Sánchez, P.-A. Hervieux, M. Alcamí, F. Martín, *Braz. J. Phys.* 36 (2006) 529.
- [70] S. Díaz-Tendero, P.-A. Hervieux, M. Alcamí, F. Martín, *Phys. Rev. A* 71 (2005) 033202.
- [71] G. Martinet, M. Chabot, K. Wohrer, S.D. Negra, D. Gardes, J.A. Scarpaci, P. Desesquelles, V. Lima, S. Díaz-Tendero, M. Alcamí, P.-A. Hervieux, M.F. Politis, J. Hanssen, F. Martín, *Eur. Phys. J. D* 24 (2003) 149.